Astron. Astrophys. 339, 897–903 (1998)

ASTRONOMY AND ASTROPHYSICS

Stellar positions from SiO masers in the Galactic center

Loránt O. Sjouwerman[1,2,3], **Huib Jan van Langevelde**[3], **and Philip J. Diamond**[4]

[1] Onsala Rymdobservatorium, S-439 92 Onsala, Sweden
[2] Sterrewacht Leiden, P.O. Box 9513, 2300 RA Leiden, The Netherlands
[3] Joint Institute for VLBI in Europe, P.O. Box 2, 7990 AA Dwingeloo, The Netherlands
[4] N.R.A.O. Array Operations Center, P.O. Box 0, Socorro, NM 87801, USA

Received 5 February 1998 / Accepted 10 September 1998

Abstract. We report on the possibility of determining milliarcsecond accurate positions (relative to Sgr A*) for 43 GHz SiO masers located at the Galactic center. The SiO masers were found in OH/IR stars in a previous Very Large Array survey. We used the Very Long Baseline Array and the phased Very Large Array in a phase-referencing scheme with a cycle time of 40 seconds. The continuum source Sgr A* is used as phase-reference source. Because of the atmospheric phase instability at 43 GHz and sensitivity considerations, only 2 sources (from 10) were detected. However, we show that reliable positions can be obtained with calculable errors, which allows one to measure the proper motion of these stars accurate to $\approx 30\,\mathrm{km\,s^{-1}}$ in 5 years.

Key words: techniques: interferometric – astrometry – stars: kinematics – stars: AGB and post-AGB – Galaxy: kinematics and dynamics

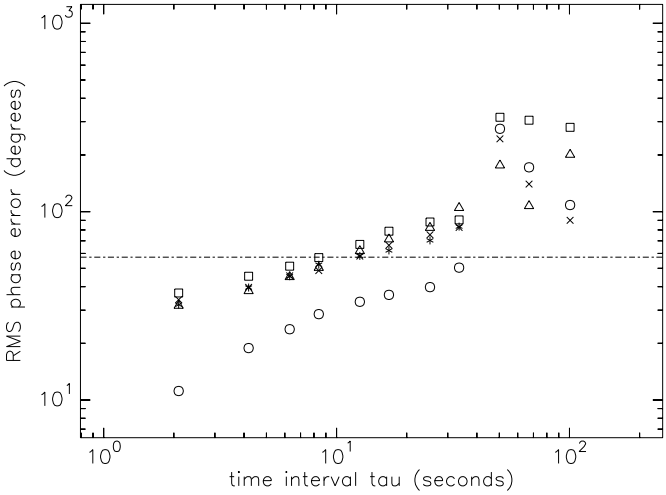

Fig. 1. RMS phase error $\sigma(\tau)$ in May 1995 for different time intervals τ. Different symbols identify different baselines. For $\tau \gtrsim 50$ seconds the proper number of cycles is more difficult to recover, resulting in an unreliable calculation of the structure function. From the plot we read a coherence time τ of about 20 seconds for the 'good' baselines on J1733−130

1. Introduction

In order to understand the nature of the central region of the Galaxy, it is crucial to have a good estimate of the mass distribution within the central parsecs of the dynamical center (Sgr A*). The most outstanding issue is that of the existence of a central massive black hole, with Sgr A* as the most likely candidate. On a larger scale, the evidence for a "bar", or a tri-axial bulge in our Galaxy accumulates. In the past decade many studies to probe the inner Galactic mass distribution have been performed, using line-of-sight velocities of gas and stars. However, because the exact type of orbits of the objects in these studies are unknown, the line-of-sight velocity information alone is of limited use. Therefore, the evidence for the existence of a massive black hole or a tri-axial bulge is heavily dependent on the assumptions made about the three-dimensional motions and the assumed potential. Genzel et al. (1994, 1997), Eckart & Genzel (1996), and Mezger et al. (1996) have reviewed the possibility of a black hole in the Galactic center (GC). Blitz et al. (1993) review the literature on the "bar" in the GC; another review is included in Morris & Serabyn (1996).

High-velocity stars ($|v_{\mathrm{LSR}}| > 250\,\mathrm{km\,s^{-1}}$) are an important constituent of the stars in the GC (Baud et al. 1975; Rieke & Rieke 1988; Van Langevelde et al. 1992a; and more recently Genzel et al. 1996). For example, Eckart & Genzel (1996) suggest that the stellar orbits in the inner parsec are isotropic in an axi-symmetric mass distribution. Hence, the high-velocity stars outline the tail of the stellar velocity distribution. On the other hand, Van Langevelde et al. (1992a) and Blommaert et al. (1998), argue that the high-velocity stars are merely bulge stars on highly elongated orbits that penetrate the center. Axi-symmetric mass distribution models are then insufficient to study the stellar dynamics of even the very center. In this case, the line-of-sight velocity dispersions – the velocity profiles – alone give a distorted picture.

Send offprint requests to: L.O. Sjouwerman (at JIVE in Dwingeloo), (sjouwerm@jive.nfra.nl)

Transverse motions

We also expect high-velocity stars in the transverse velocity domain. At the distance of the GC (8 kpc, Reid 1993), a typical stellar transverse velocity of $100\,\mathrm{km\,s^{-1}}$ corresponds to a proper motion of $\approx$ 2.5 milli-arcsecond (mas) per year. With current technology, it is possible to measure proper motions in the GC, and to deduce the type of stellar orbits with a few years of observing. Recently, Eckart & Genzel (1996) measured the proper motions of stars using near-infrared images of late-type stars in the central 0.4 parsec of the GC. However, with infrared cameras, the field of view is limited to less than one arc-minute ($\lesssim$ 2.5 parsec). We initiated a project to measure transverse velocities of OH/IR stars in the GC with VLBI. The OH/IR stars form a different sample of stars than the objects studied by Eckart & Genzel (1996) because they are located further out ($\lesssim 45'$, or $\lesssim$ 100 parsec) from Sgr A*. We assume that OH/IR stars are evolved, oxygen rich AGB stars, and refer to Iben & Renzini (1983) or Habing (1996) for further reading about AGB stars and their circumstellar envelopes.

Because of interstellar scattering in the direction of the GC, one cannot use the 1612 MHz OH masers in these OH/IR stars (Van Langevelde et al. 1992b; Frail et al. 1994). As scattering scales as λ^2, higher frequency observations are more favorable. Furthermore, it is well known that the circumstellar 43 GHz SiO masers (and 22 GHz H_2O masers) are generated closer to the star than the OH masers. The SiO masers originate from the parts of the circumstellar shell that are very close to the star (a few stellar radii with a typical diameter of $\approx$ 10 AU: Diamond et al. 1994; Miyoshi et al. 1995). Although the individual SiO maser spots are variable and are located around the star at a distance out to 5-10 AU, one can expect that the measured SiO maser position is within 10 AU of the star; i.e. the "average" spot position, which might be a blend of several of such spots, represents the stellar position within 1 mas. Also, the angular broadening due to scattering is less than 1 mas, altogether allowing a proper motion measurement of the underlying star accurate to about $30\,\mathrm{km\,s^{-1}}$ within 5 years.

Outline of this paper

We report on our efforts to obtain milli-arcsecond accurate positions for 10 SiO masers in OH/IR stars in the GC with the Very Long Baseline Array (VLBA). Because of the low elevation of the GC, the rapid phase fluctuations at 43 GHz and the low fluxes of the masers we used a special observing mode that included the phased Very Large Array (VLA) as described in Sect. 2. The resulting milli-arcsecond positions and accuracies achieved for 2 masers are given in Sect. 3. In Sect. 4. we finish with our conclusion and recommendations for future measurements.

This paper describes three sets of 43 GHz observations; the first, in May 1995, were made with the VLBA alone; the second and third were made in December 1995 and January 1996 and involved the VLBA and phased VLA. In May 1995 we also attempted to detect 22 GHz H_2O masers in OH/IR stars. However, in the subsequent observations we restricted ourselves to the 43 GHz SiO masers.

Table 1. Observational summary

		VLBA UT	VLA UT
a	1995 May 8	05^h-14^h	- -
b	1995 Dec 23	14^h-22^h	18^h00^m-20^h30^m
c	1996 Jan 12	13^h-22^h	14^h45^m-21^h45^m
Rest frequency			42.820 GHz
Total bandwidth			16 MHz
Baseband channels			2(a,c), 4(b)
Sampling rate			32 Msamp/sec with 2 bit samples
Aggregate bit rate			128(a,c), 256(b) Mbps
Spectral resolution			63(a), 125(b,c) kHz
Integration time			1 sec
Spectral weighting			uniform
Position Sgr A* (J2000):		$17^h45^m40^s.0500$	$-29°00'28''.120$

2. Observations

2.1. May 1995 - VLBA test observations

The observations in May 1995 were designated a test of 43 GHz phase-referencing techniques. For target masers we selected the brightest detections of Sjouwerman et al. (1998) lying close to Sgr A*. We used all 10 antennas of the VLBA and attempted to detect three strong SiO masers. The observational setup is described in Table 1, the antennas used are listed in Table 2. The source cycle times (the time on the reference calibrator plus the time on the maser target) was varied between 30 and 240 seconds during the run. The cycle time should be a trade-off between the atmospheric phase stability and signal to noise ratio on our $\approx$ 2 Jy, extended phase-reference source Sgr A*. For unknown reasons the Pie Town (PT) antenna failed, and bad weather affected much of the other data on the crucial short baselines of the array. Because of considerable scattering at the GC, the longer baselines were of little use for the detection of the scatter broadened masers and Sgr A*. No masers were found, but we were able to detect our intended phase-reference source Sgr A* with sufficient signal to noise for fringe-fitting in 15 second scans on the shorter baselines. For longer cycle times ($\gtrsim$ 50 seconds, Fig. 1) phase coherence was either lost, or phase referencing would leave phase ambiguities unresolved.

To estimate the coherence time in May 1995, we plotted the temporal phase structure functions (Fig. 1). For a particular baseline and time interval τ, the phase difference $\phi(t+\tau)-\phi(t)$ of the visibility phases after antenna calibration was measured (see top frame of Fig. 2). The coherence time is taken as the largest time τ for which the average RMS phase error $\sigma(\tau)$ is less than 1 radian. To calculate $\sigma(\tau)$ only short baselines on our calibrator source J1733-130 were used; Sgr A* is too weak. We find a coherence time of approximately 20 seconds for 43 GHz in the May 95 observations. We decided to use the shortest possible cycle time of 40 seconds, and to use only the inner 6 VLBA antennas in further observations.

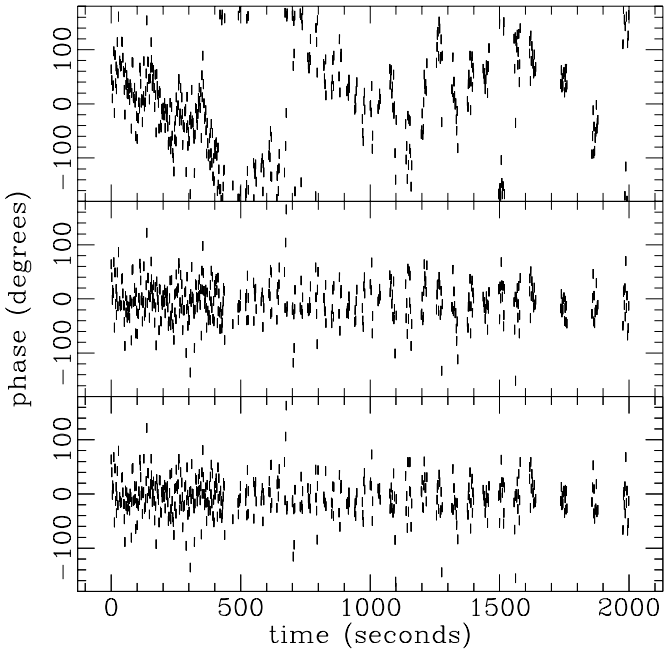

Fig. 2. Phases on a short baseline (FD-KP) for Sgr A* during a part of the 43 GHz test (May 95). The different cycle times can be seen by the source gaps: for the first $\sim$ 500 seconds the interferometer was continuously tracking Sgr A*; for the next $\sim$ 500 seconds a cycle of 15 seconds on – 15 seconds off Sgr A*was employed; during the third period of $\sim$ 500 seconds we used a cycle time of 30 seconds on – 30 seconds off Sgr A*; finally in the last period a cycle time of 30 seconds on – 90 seconds off Sgr A*was used. In the top frame we display the phases after only a-priori calibration, i.e. corrected for amplitude and a constant delay. In addition to atmospheric effects a large scatter is also caused by the low signal-to-noise ratio on Sgr A*. The middle frame displays the phases for Sgr A*, after fringe-fitting and interpolation. With a third order polynomial fit to the phases we have taken out most of the residual phase slopes and ambiguities (the bottom frame)

2.2. *VLBA and phased VLA observations - December 1995, January 1996*

The second series of experiments took place in December 1995 and January 1996, and included the phased VLA (in B-array and in transition from B- to CnB-array, respectively). The VLA proved to be crucial for this experiment, providing a) short baselines to the VLBA antennas, b) better sensitivity, and c) a contemporary check on the flux densities of the maser targets (see Sect. 3.2). In addition we used a total bit rate of 256 Msamples/s for the second epoch, increasing the sensitivity by oversampling.

The VLBA antennas are designed for fast source switching, the VLA is not[1]. Actually, it is the VLA correlator software that requires 20 seconds in between source changes and makes phase-referencing with a single VLA antenna, or with the complete VLA as one phased array for our project impractical. To circumvent this problem, the VLA was divided into two sub-arrays. One sub-array was used to observe the phase-reference source (Sgr A*), the other the maser target. The antennas were carefully divided in two interspersed sub-arrays, such that the atmospheric effects, and thus the calibration, would be comparable for each of the sub-arrays (Weiler et al. 1974). This implies that only one of the circular polarizations could be recorded for the phase-reference source, and the complementary polarization for the masers. For sensitivity reasons, we chose 5 antennas in the phase-reference array, and 8 in the maser/target one.

Every 70 minutes, all antennas were directed to J1733−130 for pointing scans and calibration. Thereafter, while the VLBA was independently performing its phase-reference schedule with a (20 + 20) second cycle time, both VLA sub-arrays were observing in simultaneous blocks of 260 seconds: 60 seconds on Sgr A* to phase up the sub-array and 200 seconds *continuously* on either Sgr A* (sub-array VLA-Ref) or a selected maser source (sub-array VLA-Mas). This complex schedule was implemented by creating a VLBA schedule that also drove the recorder at the VLA. However, the frequency and pointing setup of both VLA sub-arrays were created by hand. A summary of the observational setup is given in Table 1; the array setups can be found in Table 2.

Table 2. Array and station setup

Sub-array	Station names	Polarisation
VLBA	BR FD KP LA OV PT (+ HN MK NL SC in May 95)	Left & Right
VLA-Ref	N16 N8 E4 E12/2* W4/2*	Right
VLA-Mas	N20 N12 N4 E8 E16/6* + W16/6* W12/8*	Left

*: 'E12/2' indicates that the telescope was shifted from location E12 to location E2 in between Dec 23 and Jan 12

2.3. *Data reduction*

After the path of data editing, bandpass correction and calibration of antenna gains, a constant delay based on fringe finder observations was taken out. The resulting phases, shown in the top frame of Fig. 2, contain effects of the atmosphere, source structure and possibly the effects of an improper correlator model, including positional errors for the sources and telescopes. However, we expect that the largest effect will be atmospheric, in particular tropospheric. At 43 GHz, the absolute flux density calibration is determined with a relatively high uncertainty of about 30%. For calibration of the VLA gains, note that with a 40 second cycle time, it is essential to specifically ask for 5 to 10 second calibration entries in the log files of the VLA sub-arrays (in the "cal" files) as the default of 30 or 60 seconds is too large to calibrate the data. For the Jan 96 experiment we approximated the missing VLA sub-array system temperature by scaling Tant/Tsys with the single antenna value system temperature.

[1] Since the fall of 1996, the VLA can be used in a "Fast-Switching" mode. If available at the time of our observations, it would have enabled us to use the "full VLA", i.e. all 13 of the 27 antennas with a 43 GHz receiver, in a phase-reference scheme with cycles of 40 seconds (VLA Scientific memo 169).

Table 3. VLBA maser positions *referenced to Sgr A**

OH/IR star	Right Ascension (J2000)	Declination (J2000)
December 1995		
OH359.971−0.119	$17^h46^m00^s.95601$	$-29°01'23''.5096$
formal fit error	$0^s.00002$	$0''.0005$
reference phase ϵ	$0^s.00003$	$0''.0004$
VLA phase cal. δ	$0^s.00004$	$0''.0006$
correlator model	$0^s.00002$	$0''.0003$
total error:	$0^s.00006$	$0''.0009$
January 1996		
OH359.810−0.070	$17^h45^m26^s.35937$	$-29°08'04''.1804$
formal fit error	$0^s.00001$	$0''.0003$
reference phase ϵ	$0^s.00003$	$0''.0004$
VLA phase cal. δ	$0^s.00004$	$0''.0006$
correlator model	$0^s.00002$	$0''.0003$
total error:	$0^s.00005$	$0''.0008$

The implementation of phase-referencing with respect to Sgr A* is simply done by fringe-fitting on Sgr A*, and applying the solutions for phase, delay and rate to the maser data. To the extent that they are identical in the direction of Sgr A* and the target, all aforementioned effects can be calibrated. However, a linear phase connection using rate solutions for Sgr A* did not remove all phase ambiguities in the maser data (Fig. 2, middle frame). The bottom frame in Fig. 2 shows the slight improvement with a third order polynomial fit to the phases. The latter fit yielded the best estimates for the maser source phases (relative to Sgr A*). Following the calibration we may attempt to detect the masers *without* further (self-)calibration.

3. Results

3.1. Detections

With integration times of 30 to 60 minutes on 10 targets, 2 sources were detected. Source OH359.971−0.119 was detected in December 1995 at a SNR of 6.5 and a velocity of -10.5 ± 0.9 $\mathrm{km\,s^{-1}}$. An attempt to re-detect OH359.971−0.119 in January 1996 was unsuccessful. It was detected in the simultaneously correlated VLA data, and should therefore be detectable with the VLBA. We are convinced that the detection from December 1995 is real, as the maser can be seen consistently in two phase-referencing blocks that are more than two hours apart. In the Jan 96 experiment we detected OH359.810−0.070 at a SNR of 7.6 and a velocity of -34.1 ± 0.9 $\mathrm{km\,s^{-1}}$. We show the images for the channel with the highest peak flux in Fig. 3 and Fig. 4. Positions and velocities (Table 3) were measured from the image with the AIPS task IMFIT.

The detection of OH359.971−0.119 in Fig. 3, was obtained with a phase connection to Sgr A* over 4′.6. The phase connection for OH359.810−0.070, at a distance of 8′.2, is not as convincing as for OH359.971−0.119. Only from a detection in an adjacent channel we have a consistent position for the peak identified in Fig. 4 and quoted in Table 3. Phase referencing over 8′.2 should produce similar errors to that over 4′.6, but better understanding of this distance dependence is needed.

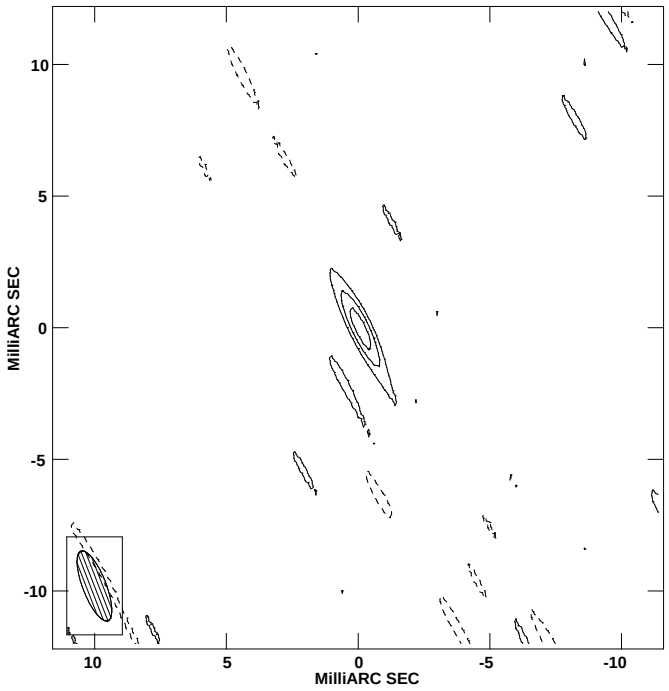

Fig. 3. Detection of OH359.971−0.119 at -10.5 $\mathrm{km\,s^{-1}}$. Contour levels are −2, 2, 4 and 6 times the RMS noise level

Table 4. "Phased" VLA maser observations and detections

Rest frequency			42.820 GHz
Correlator mode			1D
Integration time			5 sec
IF Bandwidth			25 MHz
Number of channels			32
Spectral resolution			5.5 $\mathrm{km\,s^{-1}}$
OH/IR star	Peak flux Jy	SNR	Velocity $\mathrm{km\,s^{-1}}$
December 1995			
OH359.803−0.021	(not observed)		
OH359.855−0.078	not detected		
OH359.873−0.209	(not observed)		
OH359.946−0.047	(not observed)		
OH359.971−0.119	0.17	8.0	−11
OH359.974+0.162	0.19	6.2	−27
January 1996			
OH359.762+0.120	0.28	9.0	−6
OH359.778+0.010	0.36	24.6	−27
OH359.810−0.070	0.24	16.4	−33
OH359.971−0.119	0.26	17.0	−11
OH000.142+0.026	0.11	5.2	+27

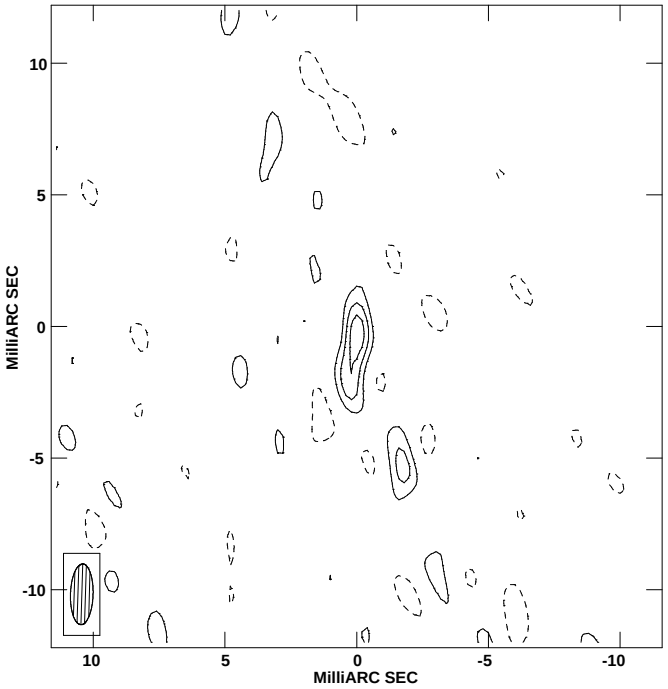

Fig. 4. Detection of OH359.810−0.070 at $-43.1\,\mathrm{km\,s^{-1}}$. Contour levels are −2, 2, 4 and 6 times the RMS noise level. Note that some of the flux is scattered into two more components The main component is also detected in an adjacent channel

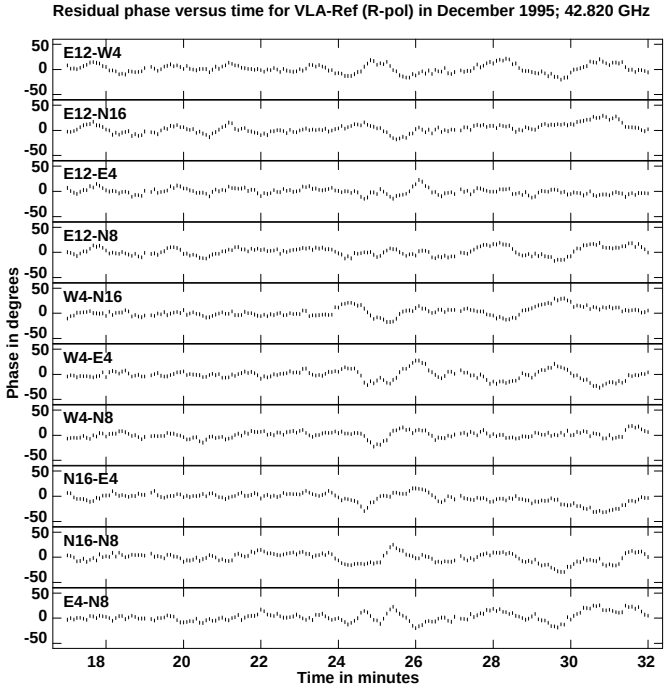

Fig. 5. Residual phase for all baselines in VLA-Ref in December 1995: first the auto-phasing mode, then from t = 24 minutes the extended-phasing mode. Note that the offsets are not entirely random for short time intervals ($\sim$ 1 minute)

3.2. Non–Detections

In the first experiment (VLBA test of May 95, without the VLA), no maser sources were detected. In the subsequent experiments, only 2 detections were obtained from 11 attempts on 10 sources. However, 7 out of 8 sources were simultaneously detected in the correlated output of the phased VLA. The VLA detections and VLA correlator setup can be found in Table 4, where we have assumed a rather low flux density of 6 Jy for J1733−130 to estimate a lower limit on the maser source flux densities. Most maser sources therefore have a flux density sufficient to detect them in the VLBI measurements as well. We conclude that the variability of the SiO maser does not explain the low VLBI detection rate.

Positional errors from the OH maser surveys can be as large as one arcsecond; a possible reason for not detecting a maser. We mainly used OH maser positions from Lindqvist et al. (1992a), which are consistent at the $1''$ level with our own SiO maser positions (Sjouwerman et al. 1998). However, Lindqvist et al. (1992a) do not give a position for Sgr A*, leaving the possibility that the positional error with respect to Sgr A* is larger than $2''$. The source would then fall outside our field of view.

However, we believe that the detection rate is mostly limited by difficulties in making a phase connection. This is partly due to atmospheric instabilities. In combination with low signal to noise on Sgr A*, it is likely that not all phase slopes have been removed in our 20 second fringe-fit interval. Recall that we observed with cycle times (40 seconds) longer than the coherence time (about 20 seconds); shorter cycles are currently impossible because Sgr A* is difficult to detect already. We conclude that it is important to observe in the best available conditions, when the atmospheric water vapour contribution is low, and possibly with larger continuum bandwidth.

3.3. Positional accuracy

It is important to make estimates of the accuracy of the measured positions. The first component in the positional uncertainty is simply the noise in the observations of the target sources. Although this determination is also affected by residual effects in the phase connection, we simply take the formal error of the fit in the map for this. This will yield a conservative estimate.

One also has to account for the uncertainty in the phase-reference calibration scheme. Ideally the residual visibility phase ϕ of the calibrator source on all baselines should be zero and without any phase slopes. Phase deviation from zero will result in a distortion of the image of the target, possibly scattering the flux of the target over multiple images. However, Fig. 2 (bottom frame) shows that the average on Sgr A* is indeed zero, albeit with a large scatter. It suffices to estimate the RMS phase error ϵ, due to noise on the reference and estimate the uncertainty on the derived position. The estimates for these errors in position can be found in Table 3.

An additional problem can originate from the VLA data. The VLA may well be a dominant factor in our results, because of its sensitivity and the short baselines it provides. Therefore it is important to check our assumption that the atmosphere over the VLA sub-arrays is identical. The maximum magnitude of

the phase error δ due to phase instabilities on a VLA baseline can be estimated from the VLA data.

At the start of the phased VLA observations, we observed J1733−130 for 8 minutes in "auto-phasing" mode and more than 5 minutes in "extended-phasing" mode (Fig. 5). In "auto-phasing" mode, the antenna phases are contineously monitored for deviations from the source model and the derived corrections are fed back into the system to form the optimal phased-array response. This method can only be applied if the source is strong and compact enough with a well determined position. For the maser sources we had to rely on extrapolating the corrections from a calibrator ("extended-phasing" mode). Fig. 5 shows the phases are generally zero for the "auto-phasing" mode data on J1733−130. However, during the "extended-phasing" mode (after $t = 24$ minutes in Fig. 5), the phase starts to drift due to uncorrected changes in the atmosphere. Nevertheless, the deviations stay well within a range of 50 degrees, sufficient to coherently average the VLA antennas.

Fig. 6 shows the measured phase error $\delta(T)$ for the J1733−130 Dec 95 observations. The maximum length T before the effect will be calibrated was 200 seconds. We see that the "auto-phasing" scans have a phase error of about 10°. Next, the average phase error in sub-array VLA-Mas is about 50% larger than for VLA-Ref in the "extended-phasing" mode. The larger extent of the VLA-Mas sub-array produces larger phase errors, because the phases and necessary corrections for the outer antennas change fastest. We take this RMS phase error as an estimate of the *maximum*, total VLA phase error and estimate the positional error for the case that the position would only be derived from VLA baselines in Table 3.

The positions given in Table 3 are positions of the source *relative* to the adopted position of Sgr A* (Table 1). Any error in the absolute position for Sgr A*, will affect the positions for the masers in Table 3. For example proper motion of Sgr A* has been inferred and is consistent with the motion of the Sun in the Galaxy (Backer & Sramek, 1982). However, for measuring proper motions with respect to Sgr A*, our primary goal, precise absolute positions are not important.

Another source of systematic error can be the processing model. We have relied on the accuracy of the VLBA correlator model to register positional information. The experiment described here offers no independent means to check this, but Reid & Menten (pers. comm.) find in a project at similar frequencies, a systematic effect of 0.3 mas introduced by inaccuracies in the troposphere model. This positional uncertainty is added to our list of errors.

Finally an intrinsic error in the *stellar position* remains because the SiO maser surrounds the stellar atmosphere at roughly 5 AU. This effect can be estimated to be on the order of 1 mas or less for 43 GHz, still much larger than the errors calculated so far.

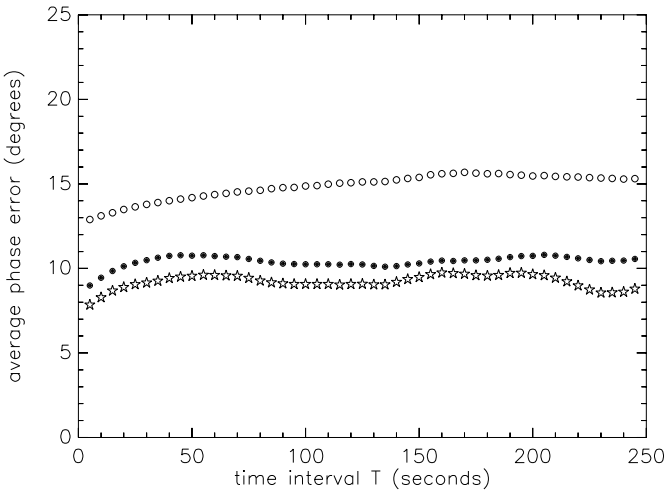

Fig. 6. Average phase error $\delta(T)$ over the VLA baselines in December 1995 over different time intervals T on the calibrator source J1733−130. The star symbols (lower line) are averages over all the "auto-phasing" scans in VLA-Ref. The filled circles are determined from the "extended-phasing" scans for VLA-Ref; the open circles are determined from the 'extended-phasing' scans in the larger sub-array VLA-Mas. VLA-Mas, which contains the maser source observations, is the relevant sub-array. The averages for the 'auto-phasing' scans for VLA-Mas lie just below the 'extended-phasing' VLA-Ref scans (filled circles) and are therefore omitted for clarity

4. Conclusions

We have successfully determined positions, relative to Sgr A*, for 2 SiO masers that are associated with AGB stars. The actual measurement is difficult because of the very rapid phase fluctuations at 43 GHz, and to a lesser extent to the variability and low quality a-priori positions of the masers. However, we have demonstrated that it is possible to obtain the positions accurately with VLBI observations, enabling future proper motion measurements. The positional errors remain within the intrinsic positional uncertainty of the location of the SiO maser in the circumstellar shell: 1 mas.

For future measurements, the Fast-Switching VLA mode will improve the sensitivity as well as reducing the phase errors compared to our experiments. However, observations need to be done under very good conditions for observing at these high frequencies and the phased VLA is essential to obtain sufficient sensitivity and short interferometer spacings. It would be advantageous to use higher bandwidth recording in the future.

Acknowledgements. We thank Bob Treuhaft and Rene Vermeulen for discussing proper cycle times. In this paper we used observations obtained with the Very Large Baseline Array (VLBA) and the Very Large Array (VLA) of the National Radio Astronomy Observatory (NRAO). NRAO is operated by Associated Universities Inc. under cooperative agreement with the National Science Foundation. For data reduction facilities LOS acknowledges the hospitality of NRAO's Array Operations Center. HJvL and LOS acknowledge support for this research by the European Commission under contract CHGECT 920011, and contract ERBFGECT 950012 respectively.

References

Backer D.C., Sramek R.A., 1982, ApJ 260, 512
Baud B., Habing H.J., Matthews H.E., O'Sullivan J.D., Winnberg A., 1975, Nat 258, 406
Blitz L., Binney J., Lo K.Y., Bally J., Ho P.T.P., 1993, Nat 361, 417
Blommaert J.A.D.L., van der Veen W.E.C.J., van Langevelde H.J., Habing H.J., Sjouwerman L.O., 1998, A&A 329, 991
Diamond P.J., Kemball A.J., Junor W., Zensus A., Benson J., Dhawan V., 1994, ApJ 430, L61
Eckart A., Genzel R. 1996, Nat 383, 415
Frail D.A., Diamond P.J., Cordes J.M., van Langevelde H.J., 1994, ApJ 427, L43
Genzel R., Hollenbach D., Townes C.H., 1994, Rep. Prog. Phys. 57, 417
Genzel R., Thatte N., Krabbe A., Tacconi-Garman L.E., 1996, ApJ 472, 153
Genzel R., Eckart A., Ott T., Eisenhauer F., 1997, MNRAS 291, 219
Habing H.J., 1996, A&AR 7, 97
Iben I., Renzini A., 1983, ARA&A 21, 271
Lindqvist M., Winnberg A., Habing H.J., Matthews H.E., 1992a, A&AS 92, 43
Mezger P.G., Duschl W.J., Zylka R., 1996, A&AR 7, 289
Miyoshi M., Matsumoto K., Kameno S., Takaba T., Iwata T., 1995, Nat 371, 395
Morris M., Serabyn E., 1996, ARA&A 34, 645
Reid M.J., 1993, ARA&A 31, 345
Rieke G.H., Rieke M.J., 1988, ApJ 330, L33
Sjouwerman L.O., Lindqvist M., van Langevelde H.J., Diamond P.J., 1998, A&A *in preparation*
van Langevelde H.J., Brown A.G.A., Lindqvist M., Habing H.J., de Zeeuw P.T., 1992a, A&A 261, L17
van Langevelde H.J., Frail D.A., Cordes J.M, Diamond P.J., 1992b, ApJ 396, 686
Weiler K.W., Ekers R.D., Raimond E., Wellington K.J., 1974, A&A 30, 241